Nonlinear Kalman filter for gyroscopic and accelerometer noise rejection of an unmanned aerial vehicle control strategy

Wassim Arfa[1], Chiraz Ben Jabeur[2], Mourad Fathallah[3], Hassene Seddik[3]

[1]Department of Electrical Engineering, Ecole Nationale d'Ingénieurs de Carthage, University of Carthage, Tunis, Tunisia
[2]Department of electrical engineering, Institue Superieur d'Informatique, University Tunis Manar, Ariana, Tunisia
[3]Department of Electrical Engineering, Ecole Nationale Supéieur d'Ingénieurs de Tunis, University of Tunis, Tunis, Tunisia

Article Info	ABSTRACT
	This study addresses timing issues inherent in traditional proportional-integral-derivative (PID) controllers for drone angle control and introduces an innovative solution, the adaptive PID flight controller, aimed at optimizing PID gains for improved performance in terms of speed, accuracy, and stability. To enhance the controller's robustness against noise and accurately estimate the system's state, a Kalman filter is incorporated. This filtering mechanism is designed to reject noise and provide precise state estimation, thereby contributing to the overall effectiveness of the adaptive PID flight controller in managing altitude dynamics for unmanned aerial vehicles (UAVs). The comparative methodology evaluates three configurations: a single PID controller for all three angles, two PID controllers dedicated to pitch/roll and yaw angles separately, and three PID sub-controllers for each angle (pitch, roll, and yaw). The study seeks to identify the most effective PID configuration in terms of stability, responsiveness, and accuracy while highlighting the added benefits of noise rejection and state estimation through the Kalman filter. This integrated approach showcases innovation and effectiveness, introducing a comprehensive solution not explored in previous research.

Corresponding Author:

Wassim Arfa
Department of Electrical Engineering, Ecole Nationale d'Ingénieurs de Carthage, University of Carthage
Tunis, Tunisia
Email: wassimarfa3@gmail.com

1. INTRODUCTION

Quadcopters, essential for high-risk tasks, utilize proportional-integral-derivative (PID) controllers for precise angle control [1]–[4]. This study proposes integrating a Kalman filter [5] before PID controllers to address noise and state estimation challenges drawing inspiration from prior research [6]–[8], it examines a 6-DOF quadcopter model, dynamic response, and PID control algorithm. Three PID controllers are dedicated to specific angles, offering a comparative analysis against single or dual controllers. Evaluation includes stability, accuracy, and disturbance avoidance, utilizing simulations and comparative techniques like genetic algorithms (GA) [9], crow search algorithm (CSA) [10], particle swarm optimization (PSO) [11], Ziegler-Nichols (ZN) [12], harmony search algorithm [13], and water cycle algorithm [14]. The integration of Kalman filter improves the control system performance and allows a more effective utilization in applications requiring precise angle control.

The paper proceeds as follows: Section 2 delves into the mathematical model based on Newton-Euler. Section 3 gives an overview of the Kalman filter characters and applications. Section 4 investigates the three applied control methods that respectively integrate the Kalman filter. Section 5 draws on the simulation

and optimization of the PID gains in the drone. The main findings and discussion are presented in Section 6. The study mainly finds out that precise tuning of the PID controller parameters is highly important to achieve optimal performance in terms of stability, responsiveness, and control accuracy. Indeed, the inclusion of three adaptive PID controllers, complemented by a Kalman filter, results in superior speed, accuracy, and stability compared to previous approaches, offering valuable insights for optimizing drones across various applications that demand precise angle control.

2.   THE MATHEMATICAL MODEL BASED ON NEWTON-EULER THEORY

This section provides a general overview of the quadcopter used in this paper, the mathematical model of the UAV, and the control structure that will accordingly be presented in Figure 1 [15]. The motors are numbered clockwise, with motor 1 at the front of the device relative to the reference frame F_b [16]. Unlike motors 2 and 4, motors 1 and 3 rotate clockwise [17].
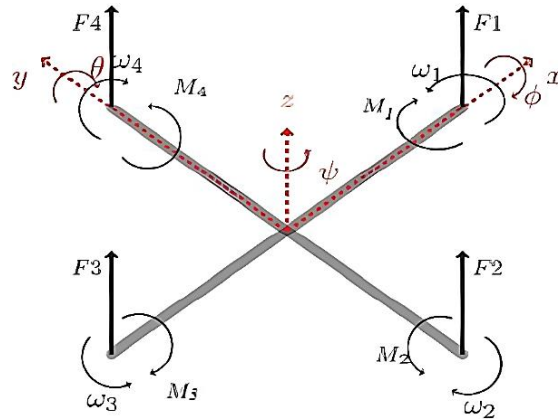

Figure 1. Direction of the rotation of rotors [17]

The equations of forces applied to the quadcopter and the moments acting on the quadrotor using the Newton-Euler formulation and the dynamic system model are shown in (1) [18],

$$\begin{cases} \dot{\zeta} = v \\ m\ddot{\zeta} = F_f + F_t + F_g \\ R = \dot{R}S(\Omega) \\ J\Omega = -\Omega\Lambda J\dot{\Omega} + M_f - M_a - M_{gh} \end{cases} \tag{1}$$

where
ζ : The vector representing the position of the quadrotor
m : The total mass of the quadrotor
Ω : The angular velocity expressed in the fixed reference frame
R : The rotation matrix
Λ : The vector product

2.1. Equations of the translational motion for drone control

After presenting the force equations in the previous sections, we can now complete the Quad-rotor model by applying Newton's second law of linear motion, as formulated in (2).

$$m\ddot{\zeta} = F_t + F_f + F_g \tag{2}$$

As we replace each force with its corresponding formula, we obtain (3).

$$m\begin{bmatrix} \ddot{x} \\ \ddot{y} \\ \ddot{z} \end{bmatrix} = \begin{bmatrix} \cos\phi\cos\psi\sin\theta + \sin\phi\sin\psi \\ \cos\phi\sin\psi\sin\theta - \sin\phi\cos\psi \\ \cos\phi\cos\theta \end{bmatrix} \sum_1^4 F_i - \begin{bmatrix} K_{ftx}\dot{x} \\ K_{fty}\dot{y} \\ K_{ftz}\dot{z} \end{bmatrix} + \begin{bmatrix} 0 \\ 0 \\ -mg \end{bmatrix} \tag{3}$$

We obtain the differential equations as (4) that define the translational coefficients.

$$\begin{cases} \ddot{x} = \frac{1}{m}(\cos\phi\cos\psi\sin\theta + \sin\phi\sin\psi)(\sum_1^4 F_i) - \frac{K_{ftx}}{m}\dot{x} \\ \ddot{y} = \frac{1}{m}(\cos\phi\sin\psi\cos\theta + \sin\phi\cos\psi)(\sum_1^4 F_i) - \frac{K_{fty}}{m}\dot{y} \\ \ddot{z} = \frac{1}{m}(\cos\phi\cos\theta)(\sum_1^4 F_i) - \frac{K_{ftz}}{m}\dot{z} - g \end{cases} \tag{4}$$

2.2. Equations of the rotational motion for drone control

Applying the same principle of Newton to the case of rotation, we get the (5)

$$J\dot{\Omega} = -\Omega \Lambda J \Omega + M_f - M_a - M_{gh} \tag{5}$$

When we replace each moment with its corresponding expression (6).

$$\begin{bmatrix} I_x & 0 & 0 \\ 0 & I_y & 0 \\ 0 & 0 & I_z \end{bmatrix}\begin{bmatrix} \ddot{\phi} \\ \ddot{\theta} \\ \ddot{\psi} \end{bmatrix} = -\begin{bmatrix} \dot{\phi} \\ \dot{\theta} \\ \dot{\psi} \end{bmatrix} \Lambda \left(\begin{bmatrix} I_x & 0 & 0 \\ 0 & I_y & 0 \\ 0 & 0 & I_z \end{bmatrix}\begin{bmatrix} \dot{\phi} \\ \dot{\theta} \\ \dot{\psi} \end{bmatrix} \right) - \begin{bmatrix} J_r\bar{\Omega}_r\dot{\theta} \\ -J_r\bar{\Omega}_r\dot{\theta} \\ 0 \end{bmatrix} - \begin{bmatrix} K_{fax}\dot{\phi}^2 \\ K_{fay}\dot{\theta}^2 \\ K_{faz}\dot{\psi}^2 \end{bmatrix} + \begin{bmatrix} lb(w_4^2 - w_2^2) \\ lb(w_3^2 - w_1^2) \\ ld(w_1^2 - w_2^2 + w_3^2 - w_4^2) \end{bmatrix} \tag{6}$$

We then obtain the differential equations defining the rotational motion as in (7).

$$\begin{cases} I_x\ddot{\phi} = -\dot{\theta}\dot{\psi}(I_z - I_y) - J_r\bar{\Omega}_r\dot{\theta} - K_{fax}\dot{\phi}^2 + lb(w_4^2 - w_2^2) \\ I_y\ddot{\theta} = \dot{\phi}\dot{\psi}(I_z - I_x) - J_r\bar{\Omega}_r\dot{\theta} - K_{fax}\dot{\theta}^2 + lb(w_3^2 - w_1^2) \\ I_z\ddot{\psi} = \dot{\phi}\dot{\theta}(I_y - I_x) - K_{faz}\dot{\psi}^2 + ld(w_1^2 - w_2^2 + w_3^2 - w_4^2) \end{cases} \tag{7}$$

with

$$\begin{cases} \ddot{\phi} = -\dot{\theta}\dot{\psi}\frac{I_z - I_y}{I_x} - \frac{J_r}{I_x}\bar{\Omega}_r\dot{\theta} - \frac{K_{fax}}{I_x}\dot{\phi}^2 + \frac{lb}{I_x}(w_4^2 - w_2^2) \\ \ddot{\theta} = \dot{\phi}\dot{\psi}\frac{I_z - I_x}{I_y} - \frac{J_r}{I_y}\bar{\Omega}_r\dot{\theta} - \frac{K_{fay}}{I_y}\dot{\theta}^2 + \frac{lb}{I_y}(w_3^2 - w_1^2) \\ \ddot{\psi} = \dot{\phi}\dot{\theta}\frac{I_y - I_x}{I_z} - \frac{K_{faz}}{I_z}\dot{\psi}^2 + \frac{ld}{I_z}(w_1^2 - w_2^2 + w_3^2 - w_4^2) \\ \ddot{x} = \frac{1}{m}(\cos\phi\cos\psi\sin\theta + \sin\phi\sin\psi)(\sum_1^4 F_i) - \frac{K_{ftx}}{m}\dot{x} \\ \ddot{y} = \frac{1}{m}(\cos\phi\sin\psi\cos\theta + \sin\phi\cos\psi)(\sum_1^4 F_i) - \frac{K_{fty}}{m}\dot{y} \\ \ddot{z} = \frac{1}{m}(\cos\phi\cos\theta)(\sum_1^4 F_i) - \frac{K_{ftz}}{m}\dot{z} - g \end{cases} \tag{8}$$

3. KALMAN FILTER

The Kalman filter, named after Rudolf E. Kálmán, is a powerful tool in estimation and signal processing and is widely used in navigation, robotics, and finance [5]. It optimizes predictions by estimating a system's hidden state amidst noise and uncertainties, enhancing accuracy through current measurements and error correction. Particularly effective in linear equations and real-time estimation, it filters out noisy information and improves state estimates. In challenging scenarios like adjusting PID controller parameters, the Kalman filter removes noise and extracts true signals for feedback. Its versatility extends to offering unbiased estimation for multi-input, non-stationary, and time-varying systems. Its recursive algorithm is well-suited for computer implementation, utilizing state equations and initial values for accurate estimation of real signal values.

$$\begin{cases} x(t) = Ax(t) + Bu(t) + Mw(t), & The\ state\ equation \\ y(t) = Cx(t) + Du(t) + v(t), & The\ mesurment\ equation \end{cases} \tag{9}$$

In the formulation of the Kalman filter, the state equation represents the system's state vector, denoted as $x(t)$, where A is the system transition matrix, $u(t)$ is the input vector, B is the control distribution matrix, and w(t) is the random Gaussian noise vector (representing system noise) characterized by a zero

mean and a known covariance structure, with M being the transition matrix for the system noise. In the measurement equation, $y(t)$ signifies the measurement vector, C is the measurement matrix, and $v(t)$ represents the measurement noise vector, which also follows a Gaussian distribution with a zero mean and known covariance structure. It is essential to note that there is no correlation between the system noise $w(t)$ and the measurement noise $v(t)$. The core objective of the Kalman filter is to estimate the true signal from a disturbed signal exhibiting a Gaussian distribution, aiming to minimize the discrepancy between the two signals.

4. OPTIMAL PID GAINS IDENTIFICATION

This section discusses the application of PID controller gains to UAVs, starting with single PID controller optimization, followed by two and three PID controllers. Existing controllers prioritize trajectory tracking performance and stability, but this can lead to higher energy consumption and reduced battery lifespan. Future controllers must consider these hidden costs along with factors like safety, reliability, and maintenance. The objective here extends beyond conventional PID control to minimize control error, reducing battery consumption and increasing autonomy. Strategies to minimize trajectory error are presented, involving manual PID gain refinement for each drone angle through an iterative process. Initial gain adjustments are made by a factor of 1 and further refined by 0.1 based on performance analysis from flight tests. This iterative and manual refinement process optimizes the control performance of the drone's altitude dynamics by precisely adjusting gains for each angle. This method involves iteratively refining PID gains for each angle of the drone, gradually enhancing stability and accuracy, and improving response to altitude command variations [19].

In this section, we discuss the PID controller, focusing on simplified models. The main objective is to design an adaptive PID controller for the flight of a Quad-rotor drone. The controller utilizes a control input, denoted as u, to regulate the position and angle of the drone according to a reference input [20]. The PID control law consists of three basic feedback control actions: proportional, integral, and derivative. The related gains are denoted as K_p, K_p, and K_d. The mathematical representation of the PID controller is in (10).

$$u(t) = \mathrm{K_p} e(t) + \mathrm{K_i} \int e(t) dt + \mathrm{K_d} \frac{\mathrm{d}}{dt} e(t) \tag{10}$$

with K_p the proportional gain, K_i the integral gain, and K_d the derivative gain, $e(t)$ can be formulated as a function of the error:

$$e(t) = s_p - p_v(t) \tag{11}$$

where s_p is the setpoint or desired position and $p_v(t)$ is the process variable at the instantaneous moment according to s_p [21]–[23].

4.1. A single PID controller optimization

Figure 2 depicts the PID controller block as a key component in the drone control loop, receiving a setpoint value and generating an output command based on error. To enhance robustness and accuracy, a Kalman filter is introduced before the PID controller, filtering noise from sensor measurements and improving state estimation. This refined state estimation allows for a more precise error assessment by the PID controller, enabling more effective utilization of its terms. With this augmented control loop, the PID controller can anticipate and correct future errors, facilitating precise setpoint attainment. The addition of the Kalman filter improves the control system's resilience to disturbances, ensuring reliable and accurate drone operation [24].
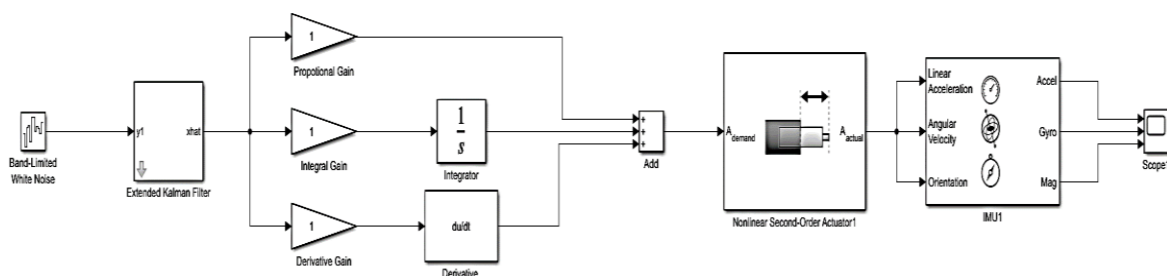

Figure 2. Control system for a single PID

The integration of a Kalman filter within the single PID controller approach for regulating all three angles of the drone serves as a crucial preprocessing step. By filtering disturbances to gyroscopes and accelerometers, it enhances estimation of the drone's state variables, addressing challenges associated with sensor measurements. This effectively mitigates noise and uncertainties, improving the control system's robustness and precision. With reduced noise influence on sensor measurements, the Kalman filter enables more accurate error computation by the PID controller. This refined error calculation leads to more reliable and stable output commands for coordinated orientation control. Thus, integrating the Kalman filter aligns with the goal of simplifying the control system while enhancing accuracy and responsiveness.

4.2. A two PID controllers' architecture

Figure 3 depicts the drone's control system with two PID blocks, PID 1 for roll and pitch, and PID 2 for yaw. PID controllers compare setpoint values to current measurements and generate output commands for motor adjustment, ensuring stable flight and precise maneuverability across all axes. The independent PID controller for yaw provides autonomous control over directional changes. To optimize controller performance, PID gains are adjusted based on drone dynamics and external conditions. Besides, a Kalman filter preprocesses data to enhance resilience against noise and uncertainties, improving overall system performance.
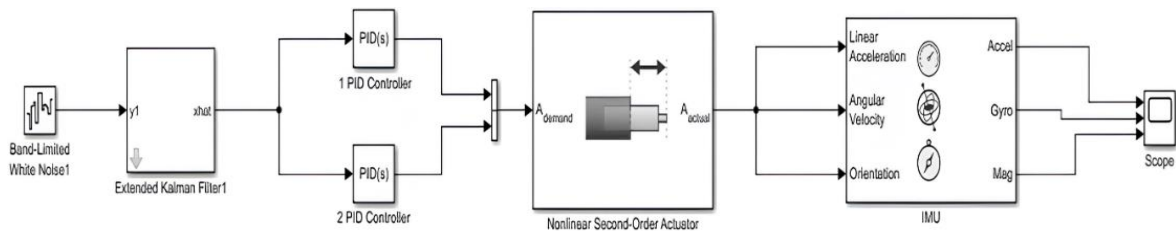

Figure 3. Control system with two PID controllers

4.3. A three PID controllers' architecture

Figure 4 illustrates a control system with three dedicated PID controllers, each regulating a specific angle of the drone. PID 1 controls roll, PID 2 controls pitch, and PID 3 controls yaw. Each controller compares desired angles to current measurements, calculates errors, and generates output commands to adjust motors accordingly. To enhance system robustness, a Kalman filter is integrated before the PID controllers, refining sensor measurements from gyroscopes and accelerometers and reducing noise and uncertainties. This refined state estimation improves error calculation accuracy by PID controllers, resulting in more precise output commands and adherence to setpoints. Thus, the Kalman filter integration enhances the control system's responsiveness and overall performance.
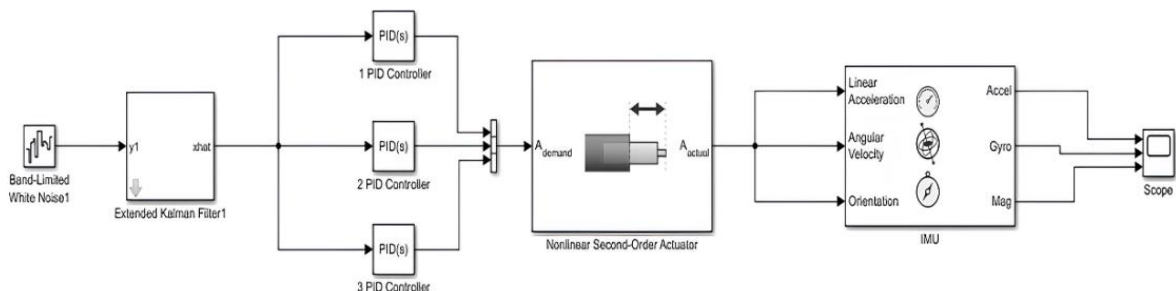

Figure 3. Control system with three PID controllers

5.   SIMULATION MODEL

This section presents simulation and experimental results evaluating the performance of the proposed PID controller design. The subsequent part includes a simulation of our control approach applied to the quadcopter dynamic model. The chosen model aims to stabilize the drone by reaching an equilibrium state with constant or zero translation coordinates and orientation angles. To achieve this purpose, PID

control is employed as the primary control technique, determining control parameters for each coordinate. Considering the digital control of the quadcopter, we opted for designing a discrete controller using MATLAB, based on the system's non-linearity. The previous and current sections offer insights into the discretization of the system performed during PID controller design based on simplified assumptions.

5.1. Model presentation and parameters

Figure 4 illustrates the complete architecture of the quadcopter simulation model in MATLAB. The model considers the quadcopter as a rigid body with a constant mass and symmetric geometry aligned with the principal axis of inertia, in a plus (+) configuration. The motors are depicted in two different colors to indicate the required synchronization that ensures the stability of the drone on the yaw axis.
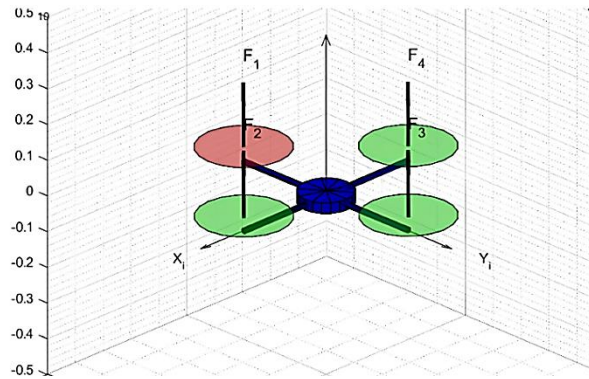

Figure 4. Quadcopter model

Table 1 lists the different parameters applied in the simulations. The physical parameters of the quadcopter are used for the simulation tests as initial conditions in the quadcopter's dynamic model. Besides, an adaptive control is developed to regulate the quadcopter's rotational dynamics.

Table 1. Parameters used in the quadcopter's dynamic model

Symbol	Description	Value	Unit
G	Acceleration due to gravity	9.81	$m.s^{-2}$
mt	Weight of the motor and propellers	0.084	kg
mq	Mass of the quadrotor	0.742	kg
At	The thickness of the arms	0.014	m
Rp	The radius of the propeller	0.127	m
Lq	Length of the quadcopter arms	0.295	m
Jx= Jy	Moment of inertia around the x and y axis	0.0163	$kg.m^2$
Jz	Moment of inertia around the z-axis	0.0326	$kg.m^2$
F1,F2,F3,F4	Motors of quadcopter	-	-

Several flight simulations were conducted to evaluate the performance of our control approach. In the first test, a single PID controller was generated for pitch, roll, and yaw angles, with carefully selected gains. The evolution of $(\vec{X}, \vec{Y}, \vec{Z})$ according to desired trajectories was examined to assess performance. In the second test, the drone was simulated with two PID controllers: one for pitch and roll, and another for yaw. Complex trajectories, including those with non-zero derivatives, were tracked to validate performance. Finally, a third PID controller dedicated to the theta angle was added to test robustness. Various performance metrics such as tracking errors, settling time, and stability were analyzed to evaluate the effectiveness and reliability of our control approach. Table 2 lists the initial conditions used for the simulations, including initial linear and angular positions. Table 3 shows the lists of parameters used in the simulation tests.

Table 2. The initial conditions for simulations

Angles	Scenario 1	Scenario 2	Scenario 3
X	0	$\frac{\pi}{2}$	0
Y	0	0	0
Z	0	0	$\frac{\pi}{2}$

Table 3. The parameters used in the simulation tests

Parameter	Value
Simulation time	10 seconds
Trajectory type	Third-order polynomial
Initial conditions	Positions, velocities, accelerations
Added noise	With white Gaussian noise

5.2. Scenario 1 analysis

In this flight simulation, tests were conducted to demonstrate the theoretical performance of the control approach. In the first test, PID controller parameters were selected and simulations were performed to observe the behavior of the control approach with a Kalman filter in the presence of noise from gyroscopes and accelerometers. This aimed to determine the role of the control function in maintaining a bounded total thrust force. Optimal PID controller gains are presented in Table 4.

Table 4. Optimal parameters for scenario 1

Angles	1 PID controller	2 PID controllers		3 PID controllers		
	All 3 angles	Pitch and Roll	Yaw	Pitch	Roll	Yaw
K_p	10.5	111.5	9	10	10	14
K_d	6	19.1	6	1	14.5	8
K_i	0.4	0.2	0.1	0.1	0.1	0.3

Figures 6 to 8 illustrate the tracking of the desired trajectory by the quadrotor during the flight simulation. Despite slight initial errors on all three axes due to noise, the quadrotor accurately follows the trajectory. Conclusions regarding pitch, roll, and yaw angles remain consistent: perturbation is minimal with three controllers, increases with two controllers, and becomes more significant with one PID controller. These observations underscore the importance of multiple PID controllers in improving stability, reducing disturbances, and minimizing angle errors in different directions. These figures highlight the benefits of employing a distributed control system capable of effectively managing multiple angles while mitigating noise effects through Kalman filtering, thereby reducing errors for each angle.
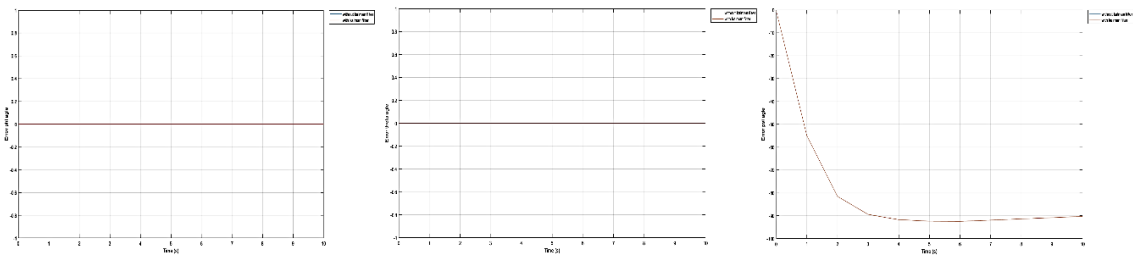

Figure 5. 1 PID controller with Kalman filter integration for Euler angle stabilization for scenario 1
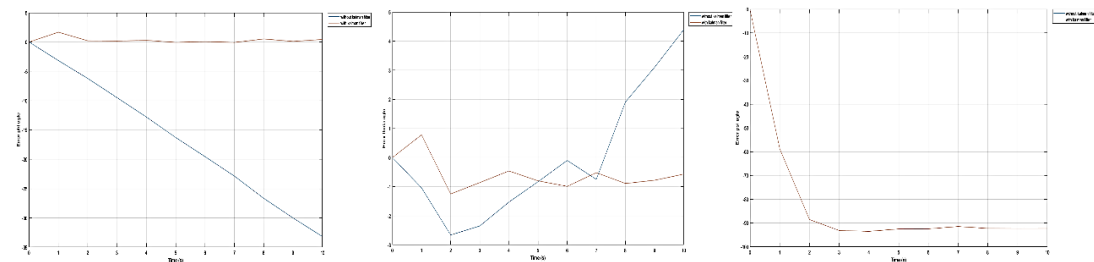

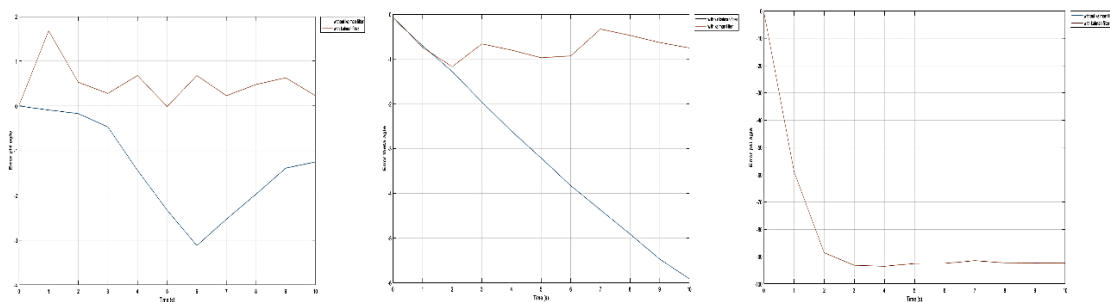Figure 6. 2 PID controllers with Kalman filter integration for Euler angle stabilization for scenario 1

Figure 7. 3 PID controllers with Kalman filter integration for Euler angle stabilization for scenario1

5.3. Scenario 2 analysis

Table 5 displays the optimal PID controller gains for the second scenario. Values are listed for roll, pitch, and yaw angles in each trial with PID 1, PID 2, and PID 3, reflecting specific results for each case. As we can observe in Figures 9 to 11, when we applied an initial condition on the $(\vec{X}, \vec{Y}, \vec{Z})$ axes $(\frac{\pi}{2}, 0, 0)$, we found similar results to those mentioned earlier. Equally for the pitch, roll, and yaw angles, the drone stabilizes faster when using three PID controllers, while it takes more time with two controllers, and even longer with just one. This observation confirms the advantage of utilizing multiple PID controllers to achieve faster stabilization and improved pitch angle performance. Essentially, employing more controllers leads to better, steadier, and quicker stabilization. Moreover, in the presence of noise from the gyroscopes and accelerometers, integrating a Kalman filter can effectively mitigate errors associated with individual angles.

Table 5. Optimal parameters for scenario 2

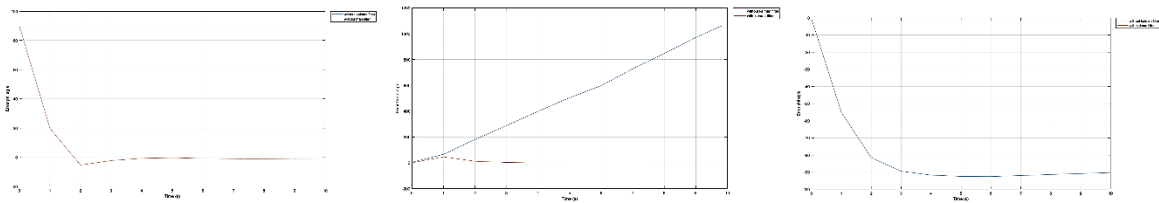| angles	1 PID controller	2 PID controllers		3 PID controllers		
	All 3 angles	Pitch and Roll	Yaw	Pitch	Roll	Yaw
K_p	9	89	9	10	110	14
K_d	8	14.5	6	1	15	7.1
K_i	0.4	0.2	0.1	0.1	0.1	0.3

Figure 9. 1 PID controllers with Kalman filter integration for Euler angle stabilization for scenario2
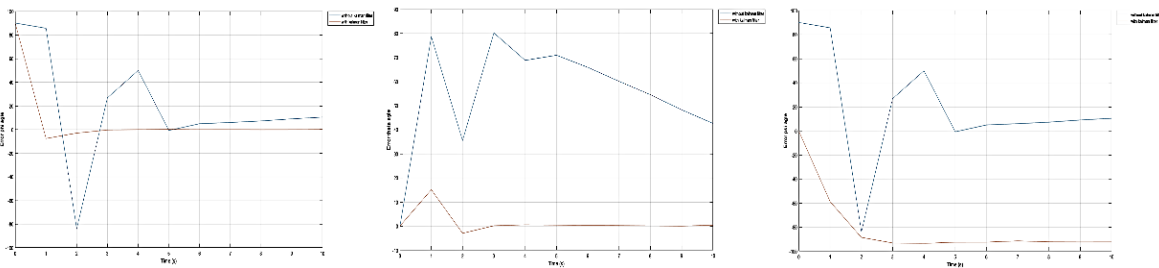

Figure 10. 2 PID controllers with Kalman filter integration for Euler angle stabilization for scenario2
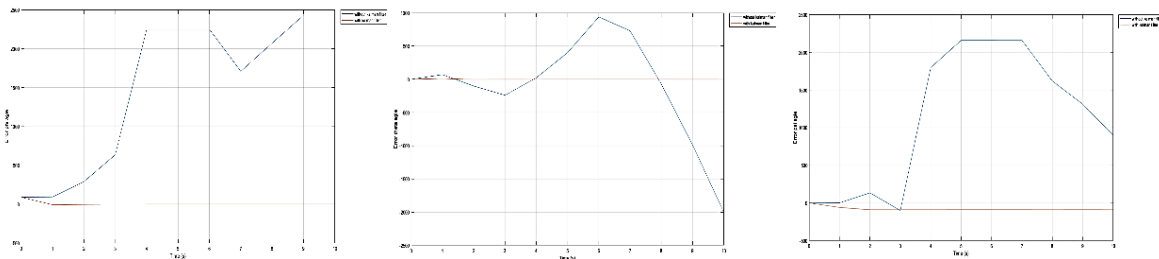

Figure 11. 3 PID controllers with Kalman filter integration for Euler angle stabilization for scenario2

5.3. Scenario 3 analysis

Table 6 outlines the optimal PID controller gains for the second scenario, detailing values for roll, pitch, and yaw angles across trials using PID 1, PID 2, and PID 3. These entries provide a specific breakdown of results for each case examined.

Table 6. Optimal parameters for scenario 3

Angles	1 PID controller	2 PID controllers		3 PID controllers		
	All 3 angles	Pitch and Roll	Yaw	Pitch	Roll	Yaw
K_p	13	89	10	10	110	14
K_d	10	14.5	7	1	15	9.1
K_i	0.4	0.2	0.1	0.1	0.1	0.1

Figures 12 to 14 depict the flying robot's tracking of the desired trajectory in three-dimensional space during flight. The observations reveal the varying performances of PID controllers for desired angles. A single controller somewhat reduces noise disturbances for pitch, roll, or yaw angles. The reduction in errors becomes more significant with two controllers, and disturbances are nearly eliminated with three controllers. Thus, employing multiple PID controllers effectively enhances stability and greatly diminishes disturbance impacts on these angles. Additionally, integrating a Kalman filter can further reduce errors associated with gyroscopes and accelerometers for each angle in the presence of noise.
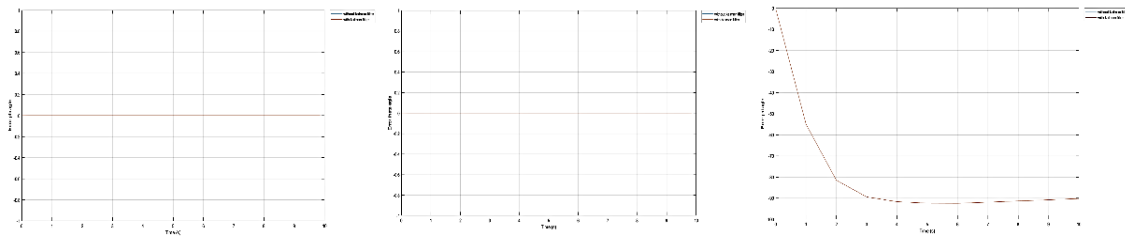

Figure 8. 1 PID controllers with Kalman filter integration for Euler angle stabilization for scenario3
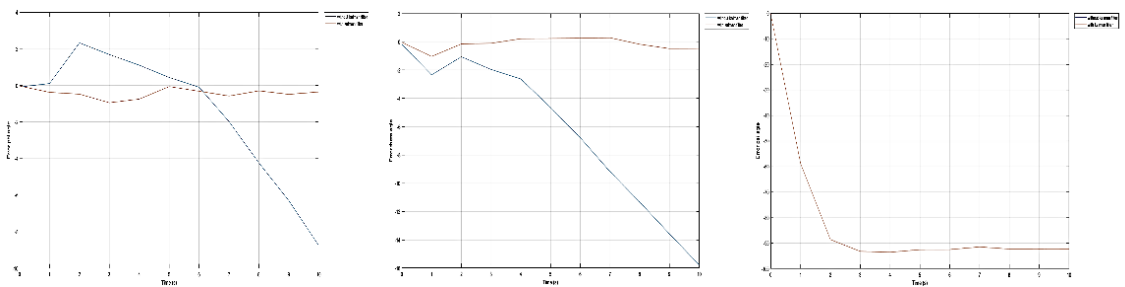

Figure 9. 2 PID controllers with Kalman filter integration for Euler angle stabilization for scenario3
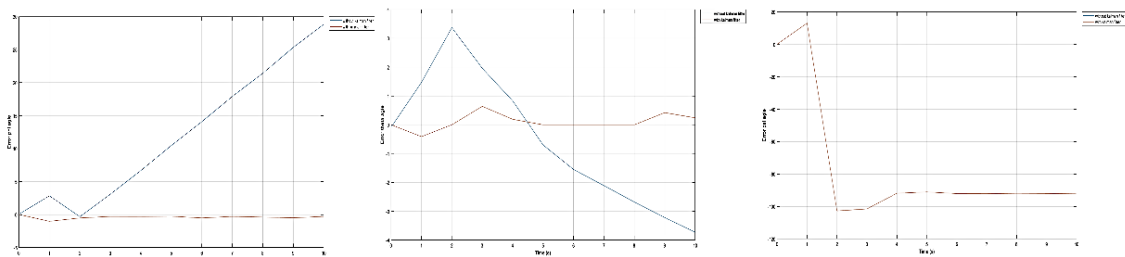

Figure 10. 3 PID controllers with Kalman filter integration for Euler angle stabilization for scenario3

6. FINDINGS AND DISCUSSION

This comparative study aimed to optimize PID gains by comparing our approach, utilizing an improved PID controller based on the Kalman filter for disturbance minimization, with other methods such as GA, CSA, PSO, and ZN tuning methods. Criteria included time stabilization and optimal PID gains. Simulations were compared to results proposed by Sheta and Alaa [24]. measuring and comparing stabilization times. Our approach achieved stabilization times between 2 and 3 seconds, shorter than others. Table 7 represents the performance of these approaches.

Table 1. The performance of the approaches in seconds (s)

Angles	1 PID Controller	2 PID controllers	3 PID controllers	ZN	PSO	CSA	GA
Roll	3	0.5	1.5	50	20	20	20
Pitch	2	1.5	1.5	40	25	40	-
Yaw	10	3	2	80	40	80	17

Through detailed analysis, we compared techniques used in each approach, noting differences that influence the stabilization time. Our manual PID gain tuning resulted in shorter stabilization times, ensuring improved responsiveness and agility. Additionally, our approach demonstrated robust stability under various conditions, unlike others that showed sensitivity to disturbances, leading to longer stabilization times [25], [26].

7. CONCLUSION

This study proposes enhancing drone control by employing a three PID controller for each angle, along with a Kalman filter as a preprocessing step. This integration improves stability, accuracy, and speed by filtering disturbances and refining control tuning. Comparative analysis demonstrates the effectiveness of the three PID controller approaches, providing better control adaptation to each angle's characteristics and improving trajectory tracking accuracy. Additionally, the Kalman filter significantly reduces noise disturbances, enabling more precise error calculation for the PID controller, particularly within the three PID controller framework. While proving to be effective, further research is warranted to optimize controller performance, potentially through refining the Kalman filter and exploring the active disturbance rejection controller for enhanced stability.

REFERENCES

[1] H. Batti, C. Ben Jabeur, and H. Seddik, "Autonomous smart robot for path predicting and finding in maze based on fuzzy and neuro-Fuzzy approaches," *Asian Journal of Control*, vol. 23, no. 1, pp. 3–12, May 2020, doi: 10.1002/asjc.2345.

[2] C. Ben Jabeur and H. Seddik, "Neural networks on-line optimized PID controller with wind gust rejection for a quad-rotor," *International Review of Applied Sciences and Engineering*, vol. 13, no. 2, pp. 133–147, Jun. 2022, doi: 10.1556/1848.2021.00325.

[3] R. Syam and Mustari, "Simulation and experimental works of quadcopter model for simple maneuver," *International Journal on Smart Material and Mechatronics*, vol. 1, no. 1, pp. 29–33, Nov. 2014, doi: 10.20342/ijsmm.2.1.33.

[4] A. Safaei and M. N. Mahyuddin, "Lyapunov-based nonlinear controller for quadrotor position and attitude tracking with GA optimization," Nov. 2016. doi: 10.1109/ieacon.2016.8067402.

[5] K. Rapp and P.-O. Nyman, "Optimization of extended kalman filter for improved thresholding performance," *IFAC Proceedings Volumes*, vol. 36, no. 18, pp. 119–124, Sep. 2003, doi: 10.1016/s1474-6670(17)34655-4.

[6] K. Khuwaja, N.-Z. Lighari, I. C. Tarca, and R. C. Tarca, "PID controller tuning optimization with genetic algorithms for a quadcopter," *Recent Innovations in Mechatronics*, vol. 5, no. 1., Apr. 2018, doi: 10.17667/riim.2018.1/11.

[7] J. Li and Y. Li, "Dynamic analysis and PID control for a quadrotor," Aug. 2011. doi: 10.1109/icma.2011.5985724.

[8] R. Fessi and S. Bouallègue, "LQG controller design for a quadrotor UAV based on particle swarm optimisation," *International Journal of Automation and Control*, vol. 13, no. 5, p. 569, 2019, doi: 10.1504/IJAAC.2019.101910.

[9] V. Gomez, N. Gomez, J. Rodas, E. Paiva, M. Saad, and R. Gregor, "Pareto optimal PID tuning for px4-based unmanned aerial vehicles by using a multi-objective particle swarm optimization algorithm," *Aerospace*, vol. 7, no. 6, p. 71, Jun. 2020, doi: 10.3390/aerospace7060071.

[10] A. Sheta, M. S. Braik, and S. Aljahdali, "Genetic Algorithms: A tool for image segmentation," May 2012. doi: 10.1109/icmcs.2012.6320144.

[11] A. Askarzadeh, "A novel metaheuristic method for solving constrained engineering optimization problems: Crow search algorithm," *Computers & Structures*, vol. 169, pp. 1–12, Jun. 2016, doi: 10.1016/j.compstruc.2016.03.001.

[12] V. V. Patel, "Ziegler-nichols tuning method: Understanding the PID controller," *Resonance*, vol. 25, no. 10, pp. 1385–1397, Oct. 2020, doi: 10.1007/s12045-020-1058-z.

[13] M. Dubey, V. Kumar, M. Kaur, and T.-P. Dao, "A systematic review on harmony search algorithm: Theory, literature, and applications," *Mathematical Problems in Engineering*, vol. 2021, pp. 1–22, Apr. 2021, doi: 10.1155/2021/5594267.

[14] A. Sadollah, H. Eskandar, H. M. Lee, D. G. Yoo, and J. H. Kim, "Water cycle algorithm: A detailed standard code," *SoftwareX*, vol. 5, pp. 37–43, 2016, doi: 10.1016/j.softx.2016.03.001.

[15] M. Elhesasy *et al.*, "Non-linear model predictive control using CasADi package for trajectory tracking of quadrotor," *Energies*, vol. 16, no. 5, p. 2143, Feb. 2023, doi: 10.3390/en16052143.

[16] S. Bouabdallah, A. Noth, and R. Siegwart, "PID vs LQ control techniques applied to an indoor micro quadrotor," 2004. doi: 10.1109/iros.2004.1389776.

[17] Tilki Umut, *Higher order sliding mode control of four rotor unmanned aerial vehicle*. 2019.

[18] P. Jaiswal, "Demystifying drone dynamics!. components although most of us are… | by percy jaiswal | towards data science," *Towards Data Science*, 2018.

[19] M. Najm, A. Younis, and F. Majeed, "Mathematical modelling and PID controller implementation to control linear and nonlinear quarter car active suspension," *Al-Rafidain Engineering Journal (AREJ)*, vol. 28, no. 2, pp. 113–121, Sep. 2023, doi:

        10.33899/rengj.2023.137327.1216.
[20]   A. Sarhan and S. Qin, "Adaptive PID control of UAV altitude dynamics based on parameter optimization with fuzzy inference," *International Journal of Modeling and Optimization*, vol. 6, no. 4, pp. 246–251, Aug. 2016, doi: 10.7763/ijmo.2016.v6.534.
[21]   S. Zouaoui, E. Mohamed, and B. Kouider, "Easy tracking of UAV using PID controller," *Periodica Polytechnica Transportation Engineering*, vol. 47, no. 3, pp. 171–177, Mar. 2018, doi: 10.3311/pptr.10838.
[22]   S. Khatoon, M. Shahid, Ibraheem, and H. Chaudhary, "Dynamic modeling and stabilization of quadrotor using PID controller," Sep. 2014. doi: 10.1109/icacci.2014.6968383.
[23]   Y. F. Chan, M. Moallem, and W. Wang, "Efficient implementation of PID control algorithm using FPGA technology," 2004. doi: 10.1109/cdc.2004.1429572.
[24]   A. Sheta, M. Braik, D. R. Maddi, A. Mahdy, S. Aljahdali, and H. Turabieh, "Optimization of PID controller to stabilize quadcopter movements using meta-heuristic search algorithms," *Applied Sciences*, vol. 11, no. 14, p. 6492, Jul. 2021, doi: 10.3390/app11146492.
[25]   I. Ullah, M. Fayaz, and D. Kim, "Improving accuracy of the kalman filter algorithm in dynamic conditions using ANN-based learning module," *Symmetry*, vol. 11, no. 1, p. 94, Jan. 2019, doi: 10.3390/sym11010094.
[26]   Y. Du, P. Huang, Y. Cheng, Y. Fan, and Y. Yuan, "Fault tolerant control of a quadrotor unmanned aerial vehicle based on active disturbance rejection control and two-stage kalman filter," *IEEE Access*, vol. 11, pp. 67556–67566, 2023, doi: 10.1109/access.2023.3291409.

BIOGRAPHIES OF AUTHORS

Wassim Arfa 🔗 is a PhD student at University of Carthage—Ecole Nationale d'Ingénieurs de Carthage (ENICar). He is a member of the research laboratory: RIFTSI at the ENSIT University of Tunis. His research interests include robotics, machine learning, and deep learning. He can be contacted at wassimarfa3@gmail.com.

Chiraz Ben Jabeur 🔗 holds a master's degree (2002) and a PhD degree in Electrical Engineering (2007). Now she is an assistant professor at the Higher Institute of Informatics (ISI) in the Department of Electrical Engineering and Computer Science. She is a member of the research laboratory: RIFTSI at the ENSIT University of Tunis. Her current research deals with systems control and artificial intelligence such as neural networks, fuzzy logic, and genetic algorithms related to mobile robots' domain. She can be contacted at chiraz.benjabeur@uvt.tn.

Mourad Fathallah 🔗 was born in Teboursouk, Tunisia in 1983. He received an M.S. degree in electronics and a Ph.D. in electrical engineering from the National Institute of Applied Science, Lyon, France, in 1989 and 2001, respectively. He has been currently working as a teacher at Tunis University since April 2005. His current research topics are FPGA-based embedded systems and multiple tiny object tracking. He can be contacted at mouradffr@gmail.com.

Hassene Seddik 🔗 is a full professor at the National Superior School of Engineers of Tunis (ENSIT). He obtained a full professor degree in the field of intelligent data filtering and securing. His current research interests include data security audio image and video processing applied in intelligent filtering, encryption, and watermarking. He is a senior member of IEEE. He is a member of the research laboratory RIFTSI at the ENSIT University of Tunis. He can be contacted at hassene.seddik@uvt.tn.